On a Cantor structure in a satellite scattering problem.

Jean-Marc Petit
CNRS, Observatoire de Nice, France

Michel Hénon
CNRS, Observatoire de Nice, France

Abstract

The phenomenon of chaotic scattering is described in the context of satellite encounters. We consider a one-parameter family of orbits obtained by starting with two satellites on circular, coplanar and close orbits. We numerically find that this family exhibits a large number of discontinuities, probably an infinite number. This phenomenon seems to be due to the existence of homoclinic and heteroclinic points of unstable periodic orbits. We model the chaotic scattering by a simple billiard: a point particle bounces on two disks and in addition is subjected to a constant acceleration. This leads to a one-parameter family with chaotic scattering. With the help of symbolic dynamics, the structure of the family can be completely elucidated.

1 Introduction

In the last few years, many studies have been carried out on the chaos in bound classical hamiltonian systems and powerful methods have been developed and applied. In contrast, less work has been done on chaos in classical scattering systems. However, for nearly twenty years, there have been numerical observations of complicated - chaotic - behavior in continuous scattering problems: classical models for inelastic molecular scattering (Rankin and Miller 1971, Gottdiener 1975, Fitz and Brumer 1979, Schlier 1983, Noid et al. 1986), satellite encounters (Petit and Hénon 1986), vortex dynamics (Eckhardt and Aref 1989), potential scattering (Eckhardt and Jung 1986, Jung and Scholz 1987). But until recently, this phenomenon had not been studied for itself.

We found this kind of behavior in a simple physical problem: the encounter of two satellites on close circular orbits around a planet (namely, Saturn). In section 2, we describe in detail the physical problem and derive the equations of motion. One would notice that the equations of motion are non integrable and contain no true singularities. In section 3, we present more precisely the chaos that appears in our problem: the asymptotic behavior of the system is discontinuous with respect to the initial parameters. Then, in section 4, we give some hints on what creates this phenomenon. In view of the numerical difficulties which were encountered in exploring this problem, a simple "model" problem was developped (Hénon, 1988) which is just complex enough to exhibit all the features we are interested in. This model is described in section 5.

2 The physical problem

The physical problem we consider is a particular case of the three body problem. Two light bodies M_2 and M_3 describe initially coplanar and circular orbits, with slightly different radii, around a heavy central body M_1. Bodies M_2 and M_3 are initially far apart, so that their mutual attraction is negligible. However, the inner body has a slightly larger angular velocity and eventually catches up with the outer body; the distance from M_2 to M_3 becomes small and their mutual attraction is no longer negligible. We shall call this an *encounter*. This study can be applied to different problems in astronomy: planetary rings dynamics, motion of coorbital satellites (Janus and Epimetheus of Saturn) or planetary formation. For convenience, M_1 will be called the *planet* and M_2, M_3 will be called the *satellites*. The difference between the radii of the initial circular orbits will be called the *impact parameter*.

Analytic approximations of the solution are available in two cases:

(i) When the impact parameter is sufficiently large, the result of the encounter is only a slight deflection of M_2 and M_3 from their previous circular orbits. These deflections can then be obtained by a perturbation theory (Goldreich and Tremaine 1979, 1980).

(ii) When the impact parameter is very small, the interaction of M_2 and M_3 produces a "horseshoe" motion: M_2 and M_3 "repel" each other azimutally and never come in close proximity. This case can also be treated by a perturbation theory (Dermott and Murray 1981, Yoder et al. 1983).

Between these two asymptotic cases, however, no theory exists, and apparently only a numerical integration of the equations of motion can give the answer. In order to have an accurate numerical study, we first reduce the equations to a simpler form: the classical set of Hill's equations. Only a brief review of this reduction will be given here; details can be found in Hénon and Petit 1986. We assume that the mass of either satellite is small compared to the mass of the planet:

$$m_2 \ll m_1, \qquad m_3 \ll m_1, \tag{1}$$

where m_i is the mass of body M_i. We assume also that the distance between the two satellites is small compared to their distance to the planet. In a zero-order approximation, the two satellites can then be considered as a single body in orbit around the planet. This orbit will be called the *mean orbit*, and will be assumed to be circular. We call a_0 the radius of the mean orbit. (The precise definition of a_0 does not matter, as long as it is nearly equal to the radii of the satellite orbits). The angular velocity on the mean orbit is

$$\omega_0 = \sqrt{Gma_0^{-3}}, \tag{2}$$

where m is the total mass of the system:

$$m = m_1 + m_2 + m_3. \tag{3}$$

We define

$$\mu = \frac{m_2 + m_3}{m}. \tag{4}$$

Let X_i, Y_i be the coordinates of body i in an inertial system. We introduce dimensionless coordinates by

$$X_i' = \frac{X_i}{a_0}, \qquad Y_i' = \frac{Y_i}{a_0}, \qquad m_i' = \frac{m_i}{m}, \qquad t' = \omega_0 t, \tag{5}$$

and for simplicity we drop the primes in what follows. In the new variables, the radius of the orbit, the angular velocity, the mass of the system, and the gravitational constant are all equal to 1. We choose the origin of time so that the two satellites are in the vicinity of $X = 1$, $Y = 0$ at $t = 0$. We introduce new coordinates ξ, η, which will be called *Hill's coordinates:*

$$\begin{aligned} X_i - X_1 &= (1 + \mu^{1/3}\xi_i)\cos t - \mu^{1/3}\eta_i \sin t, \\ Y_i - Y_1 &= (1 + \mu^{1/3}\xi_i)\sin t - \mu^{1/3}\eta_i \cos t, \qquad (i = 2, 3) \end{aligned} \tag{6}$$

We go over to new coordinates ξ^*, η^*, ξ, η, describing, respectively, the position of the center of mass and the relative position of the two satellites:

$$\xi^* = \frac{m_2\xi_2 + m_3\xi_3}{m_2 + m_3}, \qquad \eta^* = \frac{m_2\eta_2 + m_3\eta_3}{m_2 + m_3}, \qquad \xi = \xi_3 - \xi_2, \qquad \eta = \eta_3 - \eta_2. \tag{7}$$

The equations for the motion of the center of mass are linear and easily integrated (Hénon and Petit 1986). The equations of relative motion are approximately

$$\ddot{\xi} = 2\dot{\eta} + 3\xi - \frac{\xi}{\rho^3}, \qquad \ddot{\eta} = -2\dot{\xi} - \frac{\eta}{\rho^3}, \qquad \rho = \sqrt{\xi^2 + \eta^2}, \tag{8}$$

which are *Hill's equations* (Hill 1978). The error in these equations is of order of $\mu^{1/3}$. They become exact in the limit of vanishing satellite masses. Taking this limit is equivalent to zoom on the two satellites and the main effect is to repel the planet to infinity and transform circular orbits in straight lines.

The most important points to notice on these equations are:

(i) There is no parameter left in the equations (the same equations are valid in every physical case).

(ii) As is easily shown, the initial conditions for relative motion of circular orbits are given by only one parameter: the impact parameter h. Therefore, the set of solutions is a one-parameter family, and it seems reasonable to try to study it. We can even reduce the study to positive values of h because of the symmetries of the equations of motion.

Hill's equations admit the integral

$$\Gamma = 3\eta^2 + \frac{2}{\rho} - \dot{\xi}^2 - \dot{\eta}^2 \tag{9}$$

which can be called the *Jacobi integral* by analogy with the restricted problem. We can write the Jacobi integral in terms of the initial conditions:

$$\Gamma = \frac{3}{4}h^2. \tag{10}$$

We have performed a detailed study of the entire familly $0 < h < \infty$. Figure 1, taken from a collection of several hundred pictures, represents the relative motion of the two satellites. For convenience, we shall think of the special case $m_2 \gg m_3$, and identify the origin of the (ξ, η) system with the satellite M_2; the curves then simply represent the motion of M_3. An interesting feature is that the third body always escapes either upward or downward, but never stays close for ever. This is in agreement with a general result by Marchal (1977) which shows that the set of "capture orbits" is of zero measure. For a more detailed explanation of the equation of motion and of the orbits, see Hénon and Petit (1986) and Petit and Hénon (1986).

3 Chaotic scattering

The familly exhibits an interesting feature that we call "transitions". Roughly speaking, when h varies continuously, one can observe discontinuities. For given values of h, the orbit shape changes suddenly and an orbit that used to escape downward starts to escape upward, or the converse. This is the phenomenon that we want to develop now.

Consider an example. When h decreases from large values, the shape of the orbit changes continuously with h and the third body always escapes downward (first four plots of fig. 1).

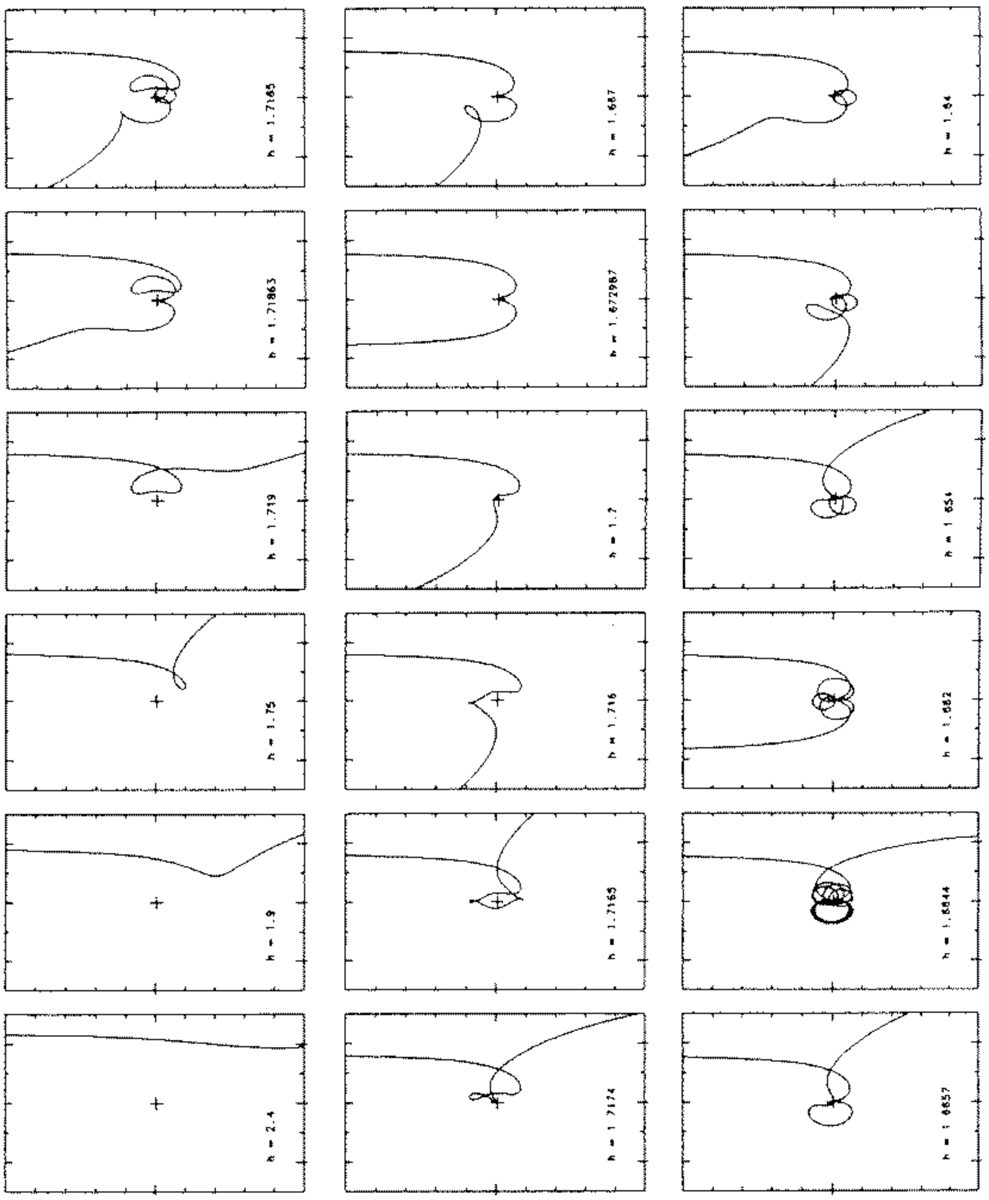

Fig. 1: Family of encounter orbits. Each frame corresponds to one particular value of the reduced impact parameter h. The curve represents the relative motion of one satellite with respect to the other, in Hill's coordinate (ξ in abscissa, η in ordinate). The first approach is downwards from $\eta = +\infty$.

Suddenly, something happens and it escapes upward. The change (transition) occurs for $h_{max} = 1.718779940$. It can be thought of as a discontinuity of the shape of the orbit. But we need a more quantitative description of this discontinuity. If we look at the equations of motion, we find that there is no true singularity in it (the $1/\rho^2$ singularity can be removed by the Levy-Cevita regularization). So the position of the third body at a given time t is a continuous function of the impact parameter h. The orbits are absolutely not chaotic. But if we look at parameters describing the asymptotic motion as functions of h, we see very sharp variations at values of h corresponding to the changes of escape side. Especially, consider the final impact parameter h' (defined from the mean motion for $t \to \infty$). Using the Jacobi integral, it can be shown that $|h'| \geq h$. In the general case of asymptotically eccentric orbits, we call k the "reduced" (transformed into Hill's coordinates) eccentricity of the relative motion. One can show that

$$\Gamma = \frac{3}{4}h^2 - k^2. \tag{11}$$

When we start with circular orbits and finish with eccentric orbits, the equality

$$\Gamma = \frac{3}{4}h^2 = \frac{3}{4}h'^2 - k'^2 \tag{12}$$

holds. Therefore, $h'^2 \geq h^2$, which leads to the previous inequality. A downward escape corresponds to $h' > 0$ and an upward escape to $h' < 0$. Therefore a change of escape side leads to a change of sign for h' and a discontinuity of step at least $2h$. This is what we mean by discontinuity. The set of discontinuity values of h being very complex, we shall speak of "chaotic" behavior of the familly.

We will now describe rapidly the set of discontinuities. Consider an orbit defined by an arbitrary value h_0. Typically, the following happens: when decreasing h from h_0, the orbit changes continuously down to h_1 where there is a discontinuity in the sense defined above. We call this a "transition value". Numerically, it is not difficult (even if time consuming) to localize this value with any accuracy. Similarly, if we increase h from h_0, we reach a second transition value h_2. The interval between h_1 and h_2 is called a "continuity interval". There are two particular cases: a continuity interval ranges from h_{max} to ∞, an other one ranges from 0 to $h_{min} = 1.336117188$ (figure 2). Suppose we have localized an interval of continuity. We do it again, starting from another value h_0 out of the range $[h_1, h_2]$. We find another interval of continuity and so on. One could expect to find all the intervals to be contiguous. This would give an exhaustive description of the orbit family.

But life is not that simple. Experiment shows that intervals are never contiguous. If one takes a point in an unexplored interval, one will find a new continuity interval which doesn't

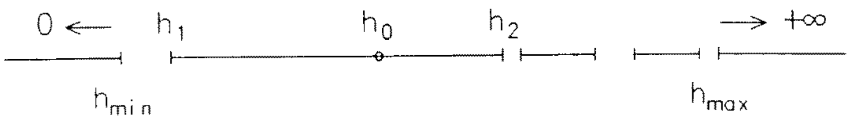

Fig. 2: A Schematic representation of the largest continuity intervals.

touch a previous interval neither on the left nor on the right. This gives birth to two new unexplored intervals. This goes on and on to infinity. One result is that there is no possible exhaustive description of the family. This must remind the reader of the classical definition of the Cantor set. The difference here is that the intervals are not regularly ordered. The actual structure can be seen on the function $h' = f(h)$ (figure 3). We can easily see the two external intervals $[0, h_{min}]$ and $[h_{max}, +\infty]$ and the three largest inner continuity intervals.

4 Some hints

We shall now try to explain how the discontinuities occur. In order to reconcile the continuity of the orbits with the discontinuity of the asymptotic behavior (h'), the family must go through an orbit with infinite capture time. This is achieved by having an orbit asymptotic to a periodic orbit. For example, figure 4 represents the transition orbit we find when decreasing h from large values: $h = h_{max}$. The orbit tends to a bean shaped periodic orbit. This limiting orbit is easily identified: it belongs to the one-parameter family a of periodic orbits, emanating from the Lagrangian point L_2 (Hénon 1969, Fig. 2). It is an unstable periodic orbit, which is necessary in a Hamiltonian system since it admits an asymptotic orbit.

It will be helpful to introduce at this point a *surface of section* defined for instance by $\eta = 0$ and $\dot{\eta} > 0$: for each crossing of an orbit with the ξ axis in the positive direction (η increasing), we plot a point with the coordinates ξ, $\dot{\xi}$ (figure 5). An orbit is then represented by a sequence of points. For a given value of Γ, a point in the surface of section defines completely the corresponding orbit: ξ, $\dot{\xi}$, η are immediately known and $\dot{\eta}$ can be computed from (9). In particular the next intersection point can be found. This defines a mapping of the surface of section onto itself, known as a *Poincaré map*.

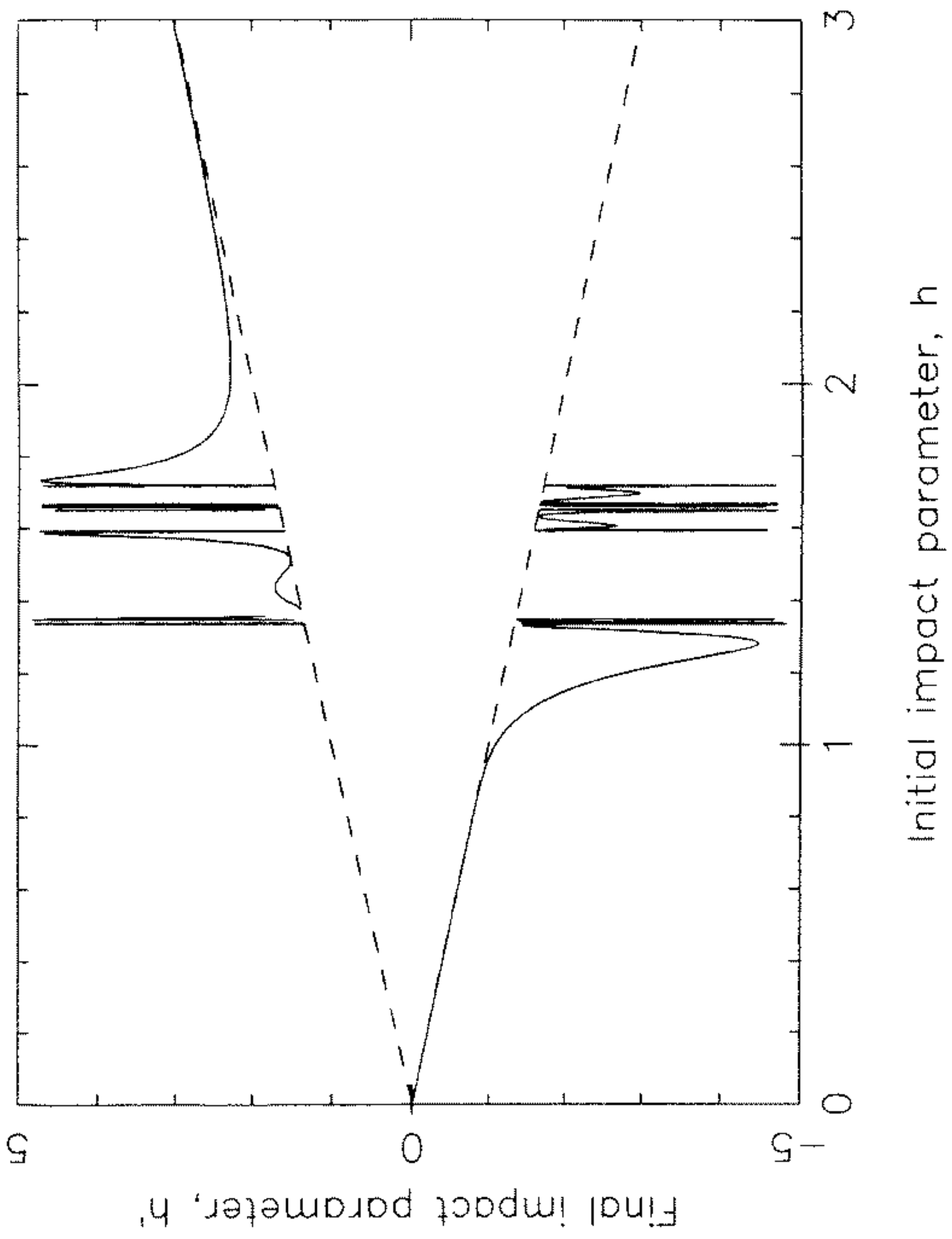

Fig. 3: Final impact parameter h' as a function of the initial impact parameter h. The region between the two dashed lines is forbidden.

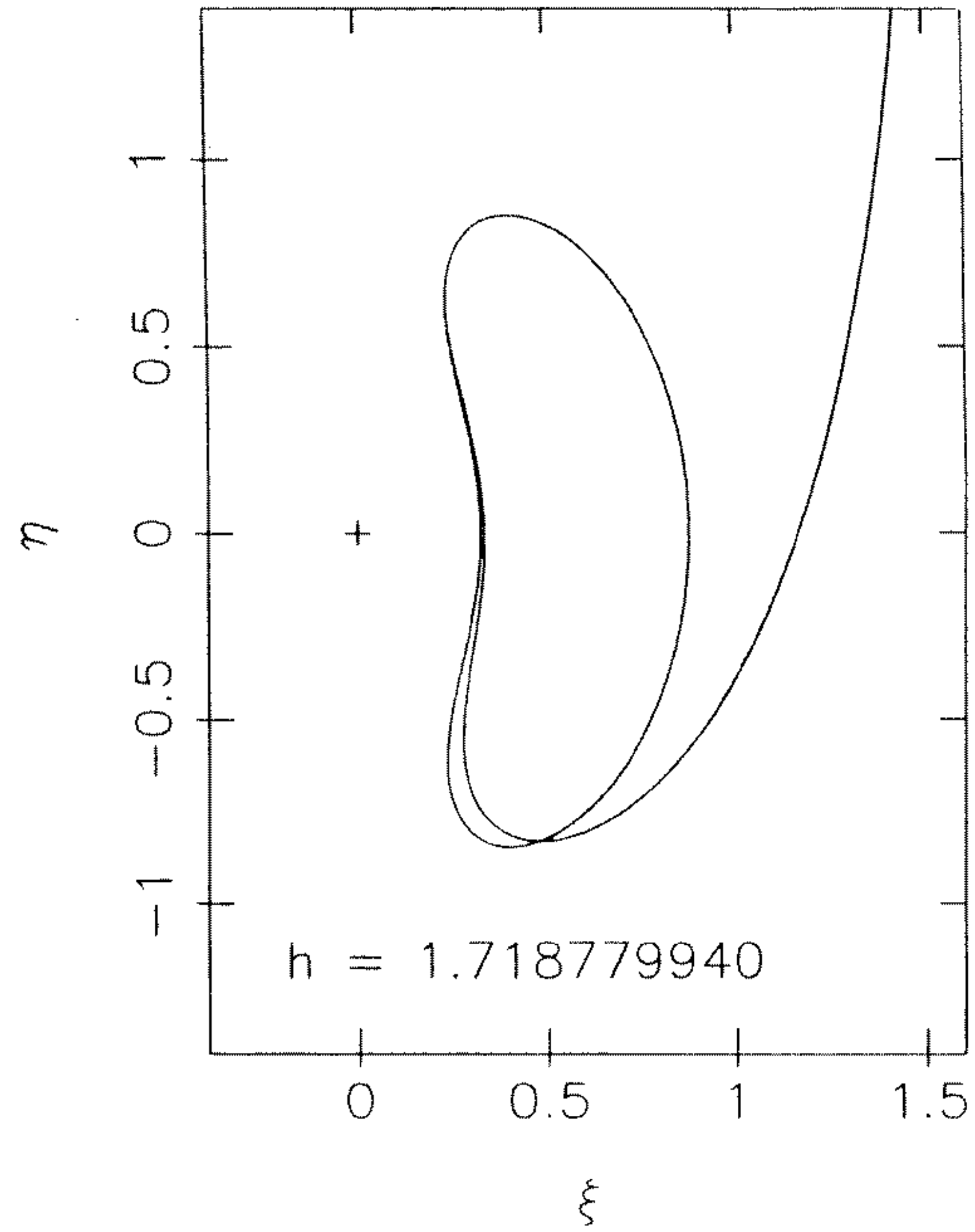

Fig. 4: An orbit of the Satellite Encounter family which is asymptotic to an unstable periodic orbit.

Note that for the orbits we are concerned with, we get generally a finite (small) number of points in the surface of section: three points for the orbit with $h = 1.71863$ for instance. An orbit can also have no point at all in that surface ($h > 2.4$). The periodic orbit is represented by a fixed point P (figure 5). The stability index of that orbit is of order 320, corresponding to two real eigenvalues $\lambda_1 = 1/640$ and $\lambda_2 = 640$. The eigenvalue smaller than 1 in modulus (λ_1) is associated with a one-parameter family of *incoming orbits* tending towards the periodic orbit. The orbit of figure 4 is a member of this family. An orbit of this family is represented by an infinite sequence of points on the *stable invariant manifold* W_s of P and converges exponentially towards P (Y_0, Y_1, Y_2, $\ldots$). Since the periodic orbit is unstable, there are also *outgoing orbits*, tending towards the periodic orbit for $t \to -\infty$. They form a one-parameter family associated with the eigenvalue larger than 1 in modulus (λ_2). They are represented by points ($\ldots$, Z_{-2}, Z_{-1}, Z_0, $\ldots$) located on the *unstable invariant manifold* W_u of P and which diverge exponentially from P.

Consider now an orbit of our family with h slightly different from h_{max}, say larger. The points in the surface of section are slightly beside W_s (crosses on the picture). They stay close to W_s until they reach the vicinity of P, then they go away along W_u. An important point is that λ_2 is positive. So the points go along only one branch of W_u. Here, it is the upper right branch. The corresponding orbits are quite regular. Particularly, they all escape downward and vary continuously when h increases (figure 6a). This accounts for the continuity interval for $h > h_{max}$.

For $h = h_{max}$, the point crosses W_s and for $h < h_{max}$, the points escape along the left branch of W_u. The two branches of W_u are in two different parts of phase space. This explains the transitions. The orbits for $h < h_{max}$ are shown on figure 6b. Things are much more complicated than before. Sometimes orbits escape upward, some time downward. So there is no continuity interval on the left of h_{max}. This explains the complex structure of the continuity intervals. For $h < h_{max}$, instead of escaping directly, the orbit will first go in the vicinity of an other unstable periodic orbit. This orbit will itself give birth to a transition phenomenon, that we shall call a *second order transition*. In this way, one can construct a hierarchical structure of transitions of higher and higher order. Suppose we have an orbit going close to one periodic orbit then close to a second one. By changing h, we can push the points in the surface of section closer to the first fixed point. Particularly, one can manage to have the same pattern along W_u and one or more additional points in the vicinity of P. This corresponds to orbits with the same escape but with one or more additional turns around the first periodic orbit (figure 7). In the first plot, the orbit follows the periodic orbit during half a turn, in the second during one and a half and in the third during two and a half (even if this is not visible one the figure). This gives rise to a geometrical progression of ratio λ_1 in the values of h.

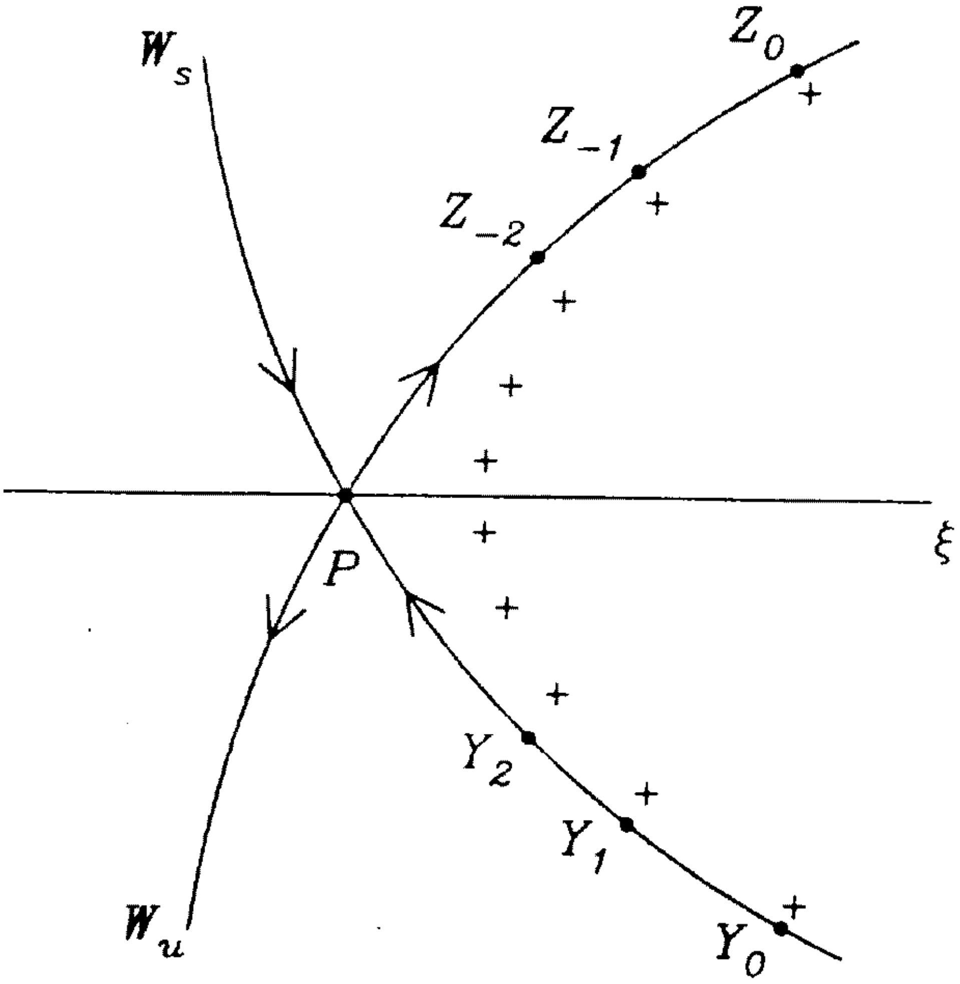

Fig. 5: Sketch of the surface of section. The value of λ_1 has been artificially increased to show the structure more clearly.

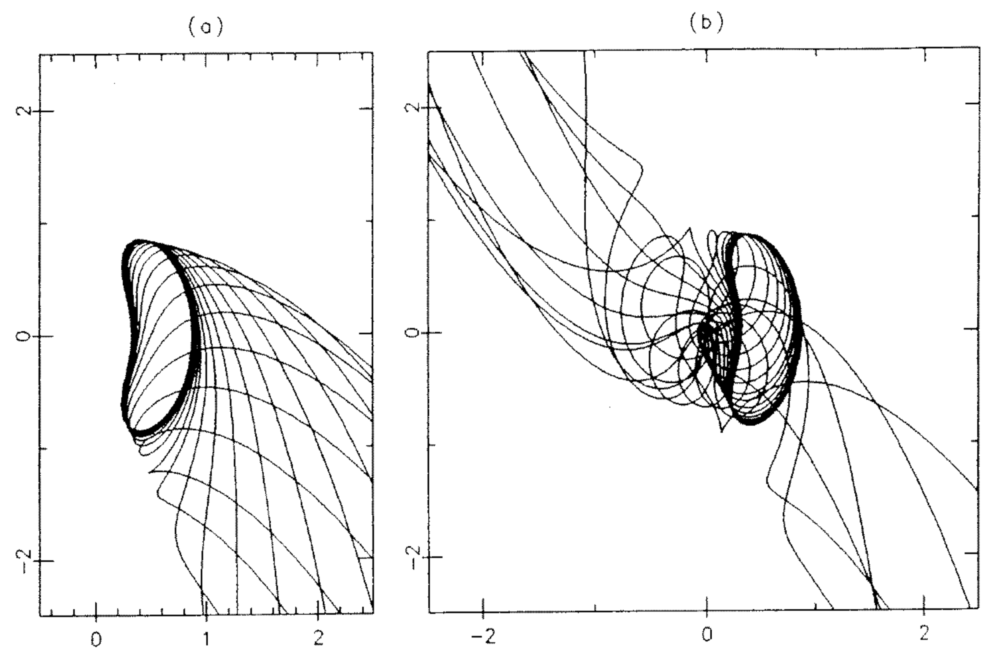

Fig. 6: (a) Outgoing orbits for h above the critical value h_{max}. (b) Outgoing orbits for h below h_{max}.

From all our numerical integrations, it seems that only two family of periodic orbits are involved: family a mentioned above and the symmetrical family b also described in Hénon 1969.

The necessary ingredients for this kind of behavior is the existence of periodic orbits and heteroclinic or homoclinic points (intersection points of invariant manifolds of two different or one single periodic orbit). But it is very difficult to go any further with this problem due to the large value of the eigenvalue (~ 640).

Other authors have observed similar behavior in scattering problems. Recently, Jung and Scholz (1988) have studied the scattering of a charged particle by a magnetic dipole. Due to the smaller value of the eigenvalue, they have been able to compute the stable and unstable manifolds of the periodic orbit with great details (solid line in Fig. 6 of their paper). It happens in their case that they need only one periodic orbit due to the presence of a homoclinic point. The dots in that figure represent the first intersection of the surface of section when varying the initial parameter. They also transported the invariant manifold into the space of initial parameters (Fig. 11 of the same paper). If now we draw a line across the figure, corresponding to the variation of one of the initial parameters, we shall see immediately the existence of a complex structure. For comparison, we did the same thing in the satellite problem (figure 8) but the structure is far too thin to be seen.

5 The inclined billiard

According to Moser (1973), in the vicinity of a homoclinic point, it is theorically possible to define a symbolic dynamics which is Bernoulli. This gives a better description of the dynamics of the system. But in our problem, we haven't been able to define it so far. So a model problem was designed which is complex enough to exhibit all the features we are interested in, and simple enough so that all the calculations can be done analytically. This model is the *inclined billiard* (Hénon, 1988). It is defined as follows: a particle moves in the (X, Y) plane and bounces elastically on two fixed disks with radius r and with their centers in $(-1, -r)$ and $(1, -r)$ respectively. In addition, it is subjected to a constant acceleration g which pulls it in the negative Y direction. To make the computation affordable, one considers the limit where r is large and approximates the circles (disks) by parabolas. The "disks" extend then from $-\infty$ to ∞ in the X direction and the number of rebounds of the particle on them is now always infinite. We suppose that initially the particle is started at (h, Y_0) where Y_0 is large. So we can neglect the thickness of the profile of the disks. Only the slopes are of consequence.

We consider the surface of section defined by the collisions. The coordinates in this surface

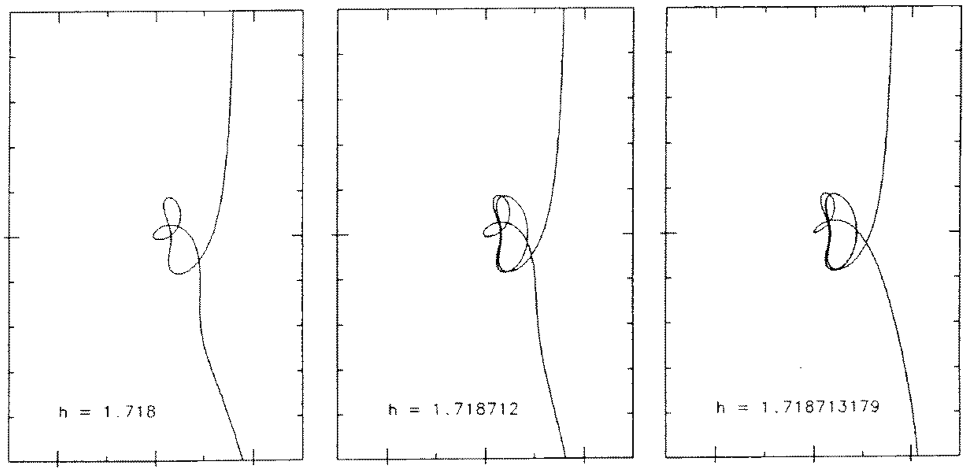

Fig. 7: Three orbits with essentially the same outgoing but different behavior during the close encounter. The orbit goes along the unstable periodic orbit for half a turn on the left, for one and a half in the middle and for two and a half on the right plot.

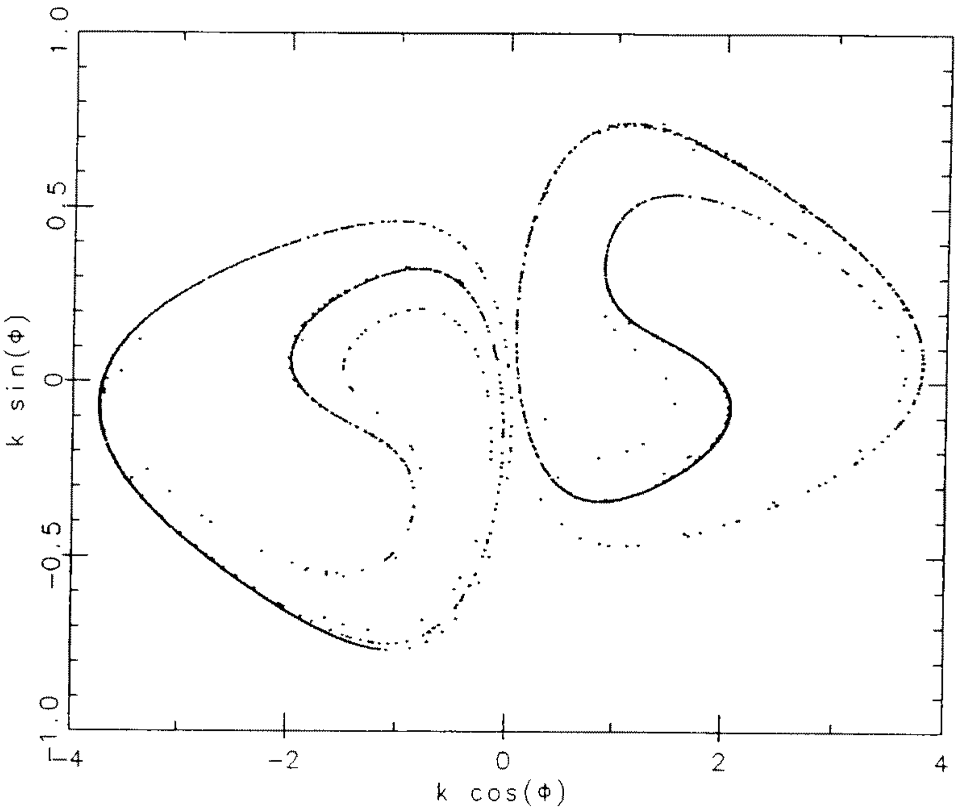

Fig. 8: Image of the invariant manifolds in the space of initial parameters.

are X, the horizontal abscissa of the collision and W, the tangential velocity of the particle. After a tedious calculation, one can finally obtain the mapping:

$$\begin{aligned}
u_{j+1/2} &= W_j + \frac{\sqrt{2E}}{r} f(X_j), \\
X_{j+1} &= X_j + \frac{2\sqrt{2E}}{g} U_{j+1/2}, \\
W_{j+1} &= U_{j+1/2} + \frac{\sqrt{2E}}{r} f(X_{j+1}),
\end{aligned} \tag{13}$$

with

$$f(X) = \begin{cases} X+1 & \text{for } X < 0, \\ X-1 & \text{for } X \geq 0, \end{cases}$$

where $U_{j+1/2}$ is the horizontal velocity between the collisions and E the energy of the particle. Arbitrarily, we have decided that the intersection of the two disks belongs to the right disk. We introduce a new parameter Φ, related to the energy by

$$\cosh\Phi = 1 + \frac{4E}{gr}, \tag{14}$$

and the new variables u and w

$$U = u\sqrt{\frac{g}{2r}\left(2 + \frac{4E}{gr}\right)}, \qquad W = w\sqrt{\frac{g}{2r}\left(2 + \frac{4E}{gr}\right)}, \tag{15}$$

in order to rewrite the mapping in a dimensionless form:

$$\begin{aligned}
X_{j+1} &= X_j \cosh\Phi + w_j \sinh\Phi - s_j(\cosh\Phi - 1), \\
w_{j+1} &= X_j \sinh\Phi + w_j \cosh\Phi - (s_j \cosh\Phi + s_{j+1}) \tanh\frac{\Phi}{2}, \\
s_j &= \text{sign} X_j.
\end{aligned} \tag{16}$$

The parameter Φ cannot be eliminated since it is related to the eigenvalue of the fixed point. It is easy to show that there are five kinds of asymptotic regimes:

1. right-escaping orbit: $X_j \to +\infty$, $w_j \to +\infty$.
2. right-asymptotic orbit: $X_j \to +1$, $w_j \to 0$.
3. left-escaping orbit: $X_j \to -\infty$, $w_j \to -\infty$.
4. left-asymptotic orbit: $X_j \to -1$, $w_j \to 0$.
5. oscillating orbit: X_j and w_j are bounded but have no limit.

We will now define a symbolic dynamics to represent the essence of the dynamics of the billiard. To each orbit we associate a semi-infinite sequence d_1, d_2, $\cdots$ of 0 and 1. The orbit is described by the sequence of points in the surface of section and each point is represented by 0 if it is a collision on the left disk and 1 if it is a collision on the right disk, rather than by its coordinates. Then we define a number A by its binary representation:

$$A = 0.d_1 d_2 d_3 \cdots = \sum_{j=1}^{\infty} 2^{-j} d_j.$$

Clearly, $0 \leq A \leq 1$. A given sequence defines one value of A, but there might be *two* sequences with the same value of A:

- If A is of the form $k.2^{-n}$, where k and n are natural numbers, A is called a round number and has two representations: $0.d_1 \cdots d_{n-1}0111\cdots$ and $0.d_1 \cdots d_{n-1}1000\cdots$.
- In the other case, A is a non-round number and the sequence is oscillating.

There is a simple correspondence between the types of orbits, the D sequence and A.

orbit	D sequence	A
right-escaping	1-ending	round
right-asymptotic	1-ending	round
left-escaping	0-ending	round
left-asymptotic	0-ending	round
oscillating	oscillating	non-round

In a continuity interval, the orbit changes continuously, so A is constant. This suggests to look at the function $A(h)$. Figure 9 shows the numerical result for $\lambda = e^{\Phi} = 3$. The reader will have recognized a *Devil's staircase.* It is possible to explain completely this figure, provided that $e^{\Phi} \geq 3$. One can show the following:

- A is a non-decreasing function of h.
- A is a continuous function of h.
- If A is non-round, it corresponds to a unique value of h defined by:

$$h = (e^{\Phi} - 1) \sum_{j=1}^{+\infty} e^{-j\Phi} s_j. \tag{17}$$

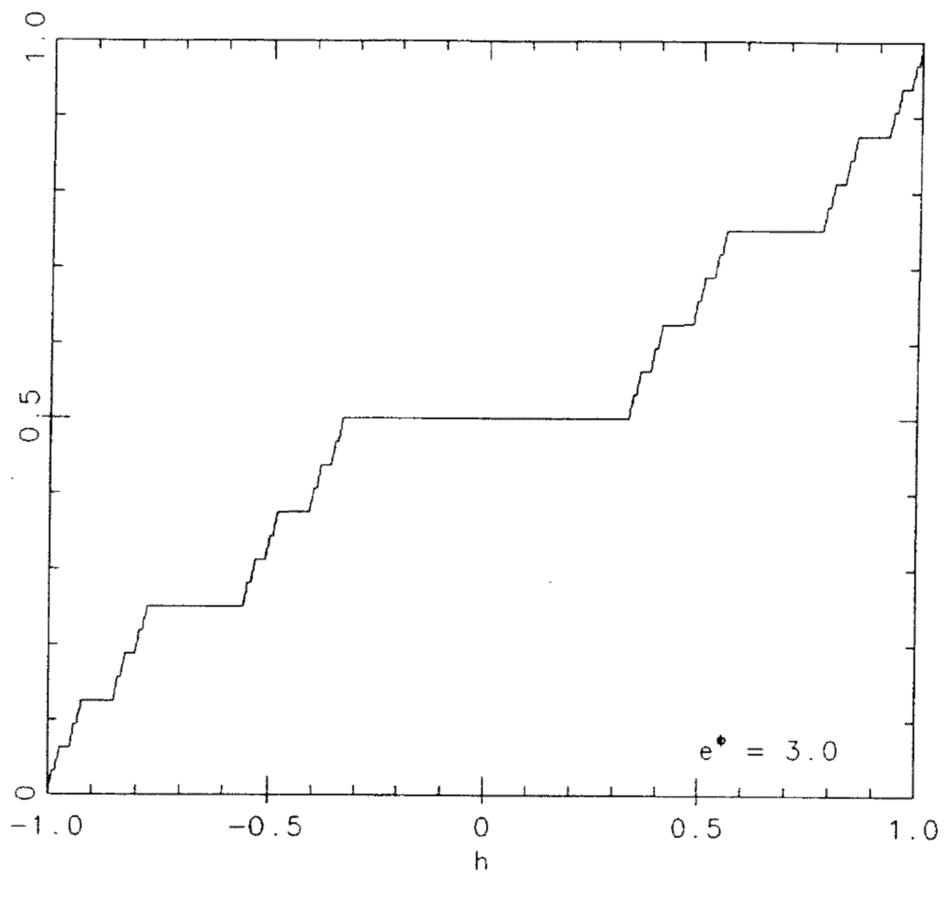

Fig. 9: The function $A(h)$ for $e^{\Phi} = 3$.

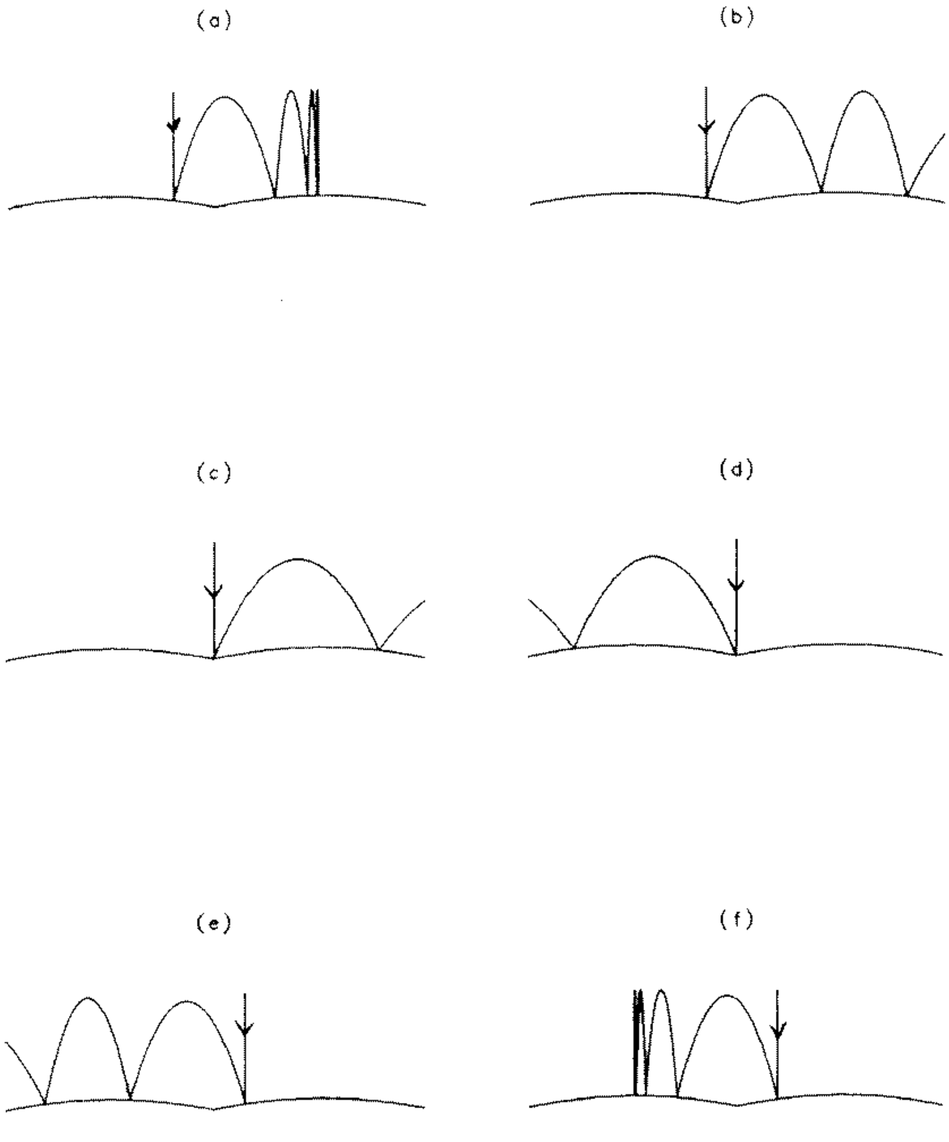

Fig. 10 Structure of the h-orbits corresponding to a round value of A (here $A = \frac{1}{2}$). (a) right-asymptotic orbit; (b), (c) right-escaping orbits; (d), (e) left-escaping orbits; (f) left-asymptotic orbit.

- If A is round, things are more interesting. A corresponds to a horizontal step, that is to a continuity interval $h_- \leq h \leq h_+$. All the steps have the same structure. Consider the central step on figure 9 (the largest). The leftmost point corresponds to an asymptotic orbit (a) (figure 10) on the right: $A = 0.0111\cdots = 1/2$. When h increases, the orbit escapes rightward and the sequence doesn't change. This is true for interval (b). After orbit (c), there is a discontinuity: the slope for the first collision changes suddenly and we go to orbit (d). Now, $A = 0.1000\cdots$, that is still $1/2$. Here, there is a small miracle: the orbit changes completely through (c) but not A. The discontinuity at $X = 0$ disappears completely in A. Then there is the interval (e) of left escaping orbits and finally the left asymptotic orbit (f). One can easily compute the values of h_- and h_+ from A:

$$\begin{aligned} h_- &= (e^\Phi - 1)\sum_{j=1}^{n-1} e^{-j\Phi}s_j - (e^\Phi - 2)e^{-n\Phi}, \\ h_+ &= (e^\Phi - 1)\sum_{j=1}^{n-1} e^{-j\Phi}s_j + (e^\Phi - 2)e^{-n\Phi}. \end{aligned} \tag{18}$$

We have thus fully solved the "inverse problem" and obtained a complete classification of h-orbits. For non-round A, there is a single h given by (17), corresponding to an oscillating orbit. For round A, there is a finite closed interval of h values $h_- \leq h \leq h_+$ (or an infinite interval in the special cases $A = 0$ and $A = 1$). This explains the *Devil's staircase* appearance of the figures.

There are two additional results that can be proved:

- The curve $A(h)$ has exact self-similarity. The curve as a whole extends from $h = -1$ to $h = +1$ and from $A = 0$ to $A = 1$. In the lower left corner is an exact replica of the whole picture, reduced by a factor e^Φ horizontally and 2 vertically, extending from $h = -1$ to $h = -1 + 2e^{-\Phi}$ and from $A = 0$ to $A = 1/2$. There is an identical replica in the upper right corner.

- The set of values of h corresponding to bounded orbits forms a Cantor set, with measure 0 and with fractal dimension

$$\ln(2)/\Phi. \tag{19}$$

  In the borderline case $e^\Phi = 3$, we obtain exactly the classical Cantor set (repeated exclusion of the middle third). The asymptotic orbits form an enumerable subset of the bounded orbits; this subset also has the dimension (19).

References

[1] Dermott S. F. & Murray C. D., 1981. Icarus **48**, p. 1.

[2] Eckhardt B. & Aref H., 1989. Phil. Trans. R. Soc. Lond. A **326**, p. 655.

[3] Eckhardt B. & Jung C., 1986. J. Phys. A **19**, p. $L829$.

[4] Fitz D. E. & Brumer P., 1979. J. Chem. Phys. **70**, p. 5527.

[5] Goldreich P. & Tremaine S., 1979. Nature **277**, p. 97.

[6] Goldreich P. & Tremaine S., 1980. Astrophys. J. **241**, p. 425.

[7] Gottdiener L., 1975. Molecular Physics **29**, p. 1585.

[8] Hénon M., 1969. Astron. Astrophys. **1**, p. 223.

[9] Hénon M., 1988. Physica D **33**, p. 132.

[10] Hénon M. & Petit J-M., 1986. Celestial Mechanics **38**, p. 67.

[11] Jung C. & Scholz H-J., 1987. J. Phys. A **20**, p. 3607.

[12] Jung C. & Scholz H-J., 1988. J. Phys. A **21**, p. 2301.

[13] Marchal C., 1977. J. Differ. Equations **23**, p. 387.

[14] Noid D. W., Gray S. K. & Rice S. A., 1986. J. Chem. Phys. **84**, p. 2649.

[15] Petit J-M. & Hénon M., 1986. Icarus **66**, p. 536.

[16] Rankin C. C. & Miller W. H., 1971. J. Chem. Phys. **55**, p. 3150.

[17] Schlier C. G., 1983. Chemical Physics **77**, p. 267.

[18] Yoder C. F., Colombo G., Synnott S. P. & Yoder K. A., 1983. Icarus **53**, p. 431.